Anal. Methods Environ. Chem. J. 7 (4) (2024) 63-77

AMECJ

Research Article, Issue 4
Analytical Methods in Environmental Chemistry Journal
Journal home page: www.amecj.com/ir

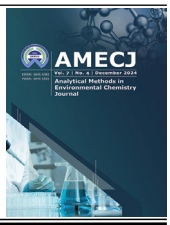

Removing textile dyes from wastewater using a novel natural polymer-based flocculant: Synthesis, characterization, and evaluation of the flocculant performance by UV-visible spectrophotometer method

Asep Nurohmat Majalis[a,*], Yosi Aristiawan[a], Bientang Matacachimi Z Sidiq[b], Fuzi Suciati[c], Vany Nursanti[d], and Andreas[a]

[a] Research Center for Chemistry, National Research and Innovation Agency, South Tangerang, Banten, Indonesia
[b] Department of Chemistry, Jendral Soedirman University (UNSOED), Purwokerto, Indonesia
[c] Research Center for Environment and Clean Technology, National Research and Innovation Agency, South Tangerang, Banten, Indonesia
[d] Research Center for Mining Technology, National Research and Innovation Agency, South Lampung, Lampung, Indonesia

ARTICLE INFO:

Received 30 July 2024
Revised form 8 Oct 2024
Accepted 17 Nov 2024
Available online 29 Dec 2024

Keywords:
Natural polymer-based flocculant,
Starch,
Chitosan,
Flocculation,
Textile dye in wastewater
UV-visible spectrophotometer

ABSTRACT

Natural polymer-based flocculants have become a promising option for wastewater treatment to replace Fe and Al-based coagulants and synthetic polymer-based flocculants. This research introduces a novel flocculant, namely Stc-EGDMA-Cts, that can act as a coagulant and a flocculant. The characteristics of Stc-EGDMA-Cts were obtained, and its effectiveness in eliminating textile dye from wastewater was evaluated using the UV-visible spectrophotometer method. The change of Stc: Cts mass ratio from 0.5 to 8 g g^{-1} increased the zeta potential value and the yield percent of Stc-EGDMA-Cts from 23.1 to 46.4 mV and 15.64 to 59.93%, respectively. Specifically, Stc-EGDMA-Cts with Stc: Cts mass ratio of 0.5, 1, 2, and 4 g g^{-1} removed textile dye from wastewater by 91.01, 92.26, 92.84, and 80.85%, respectively. However, Stc-EDGMA-Cts with a Stc: Cts mass ratio of 8 g g^{-1} could only remove less than 20%. The Stc-EGDMA-Cts performance in removing dye was also affected by the initial pH of wastewater, the Stc-EGDMA-Cts dosage, and the sedimentation time. Characterization and flocculation test results suggest that the possible mechanisms of flocculation by Stc-EGDMA-Cts are charge neutralization, adsorption, and inter-polymer linking.

1. Introduction

Water quality is essential for human life, affecting health and the economy. The contamination of the water itself is an inevitable consequence of human civilization. The analytical methods used to identify and quantify hazardous contaminants in water, such as organic materials and heavy metals, are crucial for monitoring and assessment. Gas chromatography (GC) is one of the analytical methods that can be employed to detect organic pollutants, as evidenced by the use of GC-MS and GC-FID instruments [1-4]. In parallel with establishing traditional and advanced analytical methods to monitor water quality, developing materials to remove or extract hazardous chemicals in water to produce a more beneficial water source is becoming a research concern. Teimoori et al. studied the removal of benzene,

*Corresponding Author: Asep Nurohmat Majalis
Email: asep039@brin.go.id
https://doi.org/10.24200/amecj.v7.i04.344

ethylbenzene, toluene, and xylene contaminants from water samples using a carbon nanostructure, functionalized multi-walled carbon nanotubes, and modified graphene oxide [3,5,6]. There is a growing interest in the flocculation technique as an alternative method for removing contaminants in water and wastewater [7]. Flocculation is commonly employed in wastewater treatment to eliminate heavy metals or dyes due to its convenient handling, high effectiveness, minimal energy usage, and low initial expenses [8,9]. Flocculants are utilized to rapidly divide solids and liquids by inducing colloidal particles to aggregate in a process called flocculation [8,10]. Two categories of flocculants exist: inorganic coagulants like iron and aluminum salts and organic flocculants comprising synthetic organic and natural polymer-based flocculant [11–13]. Unfortunately, secondary pollution can happen when leftover substances from aluminum and iron coagulants and synthetic polymer flocculants such as polyacrylamide are present in treated water or wastewater [14,15]. Aluminum residue has been linked to Alzheimer's disease [16,17], whereas iron residue can lead to the corrosion of metal equipment, decreasing its lifespan and increasing the expenses of wastewater treatment [18]. Polyacrylamide and other synthetic polymers could potentially be harmful to the environment because of their toxic and carcinogenic properties [18]. Furthermore, natural decomposition is difficult to achieve with synthetic polymers [19]. Natural polymers show potential as effective flocculants for treating wastewater [20]. Cellulose, chitosan, tannin, and starch are natural polymers with chemical structures and functional groups that can efficiently disrupt pollutants in wastewater [18,21,22]. Cellulose and chitosan have demonstrated high flocculation efficiency in removing textile dyes and heavy metals from wastewater because of their amino and polysaccharide functional groups, hydrophobicity, polyfunctionality, reactivity, and complexing properties. At the same time, tannin and starch showed good flocculation ability in removing anionic and cationic dye dispersions [11,21,23]. Moreover, polymers made from natural substances are cheaper and more sustainable but less harmful, able to decompose, and compatible with living organisms [18,24]. The mechanisms of flocculation by natural polymers based on flocculants are divided into six categories: neutralization of particle charge, inter-polymer bridging, charge patching, net trapping, sweeping, and adsorption [8,18,21]. Based on these mechanisms, polymer grafting can improve the performance of natural polymers as flocculants [8,25]. The grafting can produce a higher molecular weight due to the new branch in the primary molecular chain [26,27]. The grafting can combine functional groups from different compounds that have superiority in binding pollutants from wastewater. The benefits of grafting natural polymers are synergistically efficient at low doses, low cost, shear resistant, produces less sludge after the sedimentation process, biodegradable, regeneration performance, high molecular weight, no require additional coagulant, longer molecular chain, and fast sedimentation [24,28]. The grafting of starch or chitosan with a monomer or binary polymer has been widely studied and proven to improve flocculation performance [15,21,29,30]. However, the grafting of starch-monomer-chitosan or ternary polymer to produce a flocculant still needs to be improved. It is thought that grafting starch-monomer-chitosan produces a flocculant that brings the advantages of each component; chitosan is excellent in reducing heavy metals, and starch is superior in reducing dyes [21,31–33]. Starch is an abundant material consisting of a mixture of amylopectin and amylase with many hydroxyl groups in its molecular chain structure [34].Chitin deacetylation produces chitosan, a linear copolymer containing D-glucosamine and N-acetyl-D-glucosamine, along with hydroxyl and amino functional groups [27,35,36]. The mass ratio determines the impact of grafted natural polymers on inducing flocculation. The ratio of the crosslinker dose, the crosslinking temperature,

and the reaction duration [10,37]. Additionally, You and colleagues [10] found the best conditions for the effectiveness of the cationic starch/chitosan crosslinking-copolymer, with key factors being mass ratios of 4 to 5 g g^{-1} for cationic starch to chitosan, a crosslinker dosage ratio of 0.75 mg g^{-1} to cationic starch, a crosslinking temperature of 70 ºC, and a reaction time of at least 1.5 hours.

This research studied the synthesis of natural polymer-based flocculant, the starch-ethylene glycol dimethacrylate-chitosan or Stc-EGDMA-Cts, and its performance in removing dyes from wastewater. Stc-EGDMA-Cts was prepared via free radical polymerization under hydrothermal conditions, with varied mass ratios of starch to chitosan or Stc: Cts mass ratio (g g^{-1}). The characteristics of Stc-EGDMA-Cts were evaluated using Fourier transform infrared (FTIR) spectroscopy, X-ray diffraction (XRD), scanning electron microscopy (SEM), and zeta potential analyzer. The effectiveness of Stc-EGDMA-Cts in removing dye was evaluated using the UV-visible spectrophotometer method. Furthermore, the effect of the initial pH of textile dye wastewater, the Stc-EGDMA-Cts dosage, and the sedimentation time on flocculant performance was investigated.

2. Material and Methods

2.1. Materials

Soluble starch (CAS No.: 9005-84-9), EGDMA (CAS No.: 97-90-5), acetic acid (CAS No.: 64-19-7), sulfuric acid (CAS No.: 7664-93-9), sodium hydroxide (CAS No.: 1310-73-2), and azobisisobutyronitrile or AIBN (CAS No.: 78-67-1), all in analytical grade, were purchased from Sigma-Aldrich Canada Co. Low molecular weight chitosan (CAS No.: 9012-76-4) with a degree of deacetylation of 75%, and a maximum limit of impurities of 10% was purchased from Central Drug House (CDH) India. In analytical grade, Acetonitrile (CAS No. 75-05-8) and ethanol (CAS No. 64-17-5) were obtained from Merck. Professional Fabric Dyes Ltd obtained Dypro multi-purpose dye 19 deep blue or Dypro 19 (product code: 0101603119).

2.2. Instruments

The synthesis process of Stc-EGDMA-Cts was supported with an autoclave (Thermo Fisher Scientific, USA), an oven (Thermo Fisher Scientific, USA), and a centrifuge (Eppendorf, Germany). Characterization of both the raw material and Stc-EGDMA-Cts was performed by FTIR spectroscopy (Bruker-Tensor II, USA) for the study of functional groups, X-ray diffraction with a Copper (Cu) X-ray source (Malvern Panalytical AERIS, UK) for the evaluation of physical properties, SEM (PhenomProX Desktop Scanning Electron Microscope, Thermo Fisher Scientific, USA) for the analysis of surface morphology. A zeta potential analyzer (Horiba SZ 100, Japan) was employed to measure the zeta potential (ζ) of the dispersed material of Stc-EGDMA-Cts obtained from synthesis. Jar test experiments were conducted using the FC6S Jar Test instrument (VELP Scientifica, Italy). A digital pH meter (Hanna HI 2002, ITM, Canada) was used in this study. A single-beam UV-visible spectrophotometer (Agilent Cary 60 UV-Vis, USA) equipped with a 1 cm quartz cuvette was used for the dye analysis carried out in this work. A digital microscope VHX-5000 series (Keyence, Japan) was used to image the settled flocs from the jar test experiment.

2.3. The synthesis of Stc-EGDMA-Cts

Stc-EGDMA-Cts was synthesized through dissolution, mixing, homogenization, and free radical polymerization under hydrothermal conditions. A starch solution containing 2% starch by weight was blended with EGDMA (at a ratio of 0.7 mLg^{-1} of starch) at 850 rpm for 15 minutes at ambient temperature. A mixture was prepared with Stc: Cts ratios of 0.5, 1, 2, 4, and 8 g g^{-1} by adding 2% (w/v) chitosan solution in acetic acid 1% and mixing at 850 rpm for 30 minutes at room temperature. The AIBN initiator was subsequently added to the mixture (AIBN: starch mass ratio 0.8% g g^{-1}) and mixed at 850 rpm for 60 minutes at 60 ºC. Finally, the mixture was placed into an autoclave and then polymerized under

hydrothermal conditions at 90 ºC for 5 hours in the oven. The solid of Stc-EGDMA-Cts was obtained by settling a polymerized mixture for 48 hours at room temperature after adding ethanol (ethanol: starch ratio of 2.5 mLg^{-1}), followed by centrifugation at 6500 rpm for 25 minutes, filtration, and finally drying at 50 ºC for 12 hours. The yield (%) of Stc-EGDMA-Cts was calculated by Equation 1:

$$\text{Yield (\%)} = \frac{W_p}{W_c} * 100 \quad \text{(Eq.1)}$$

where W_p is the weight of the product (Stc-EGDMA-Cts) (g), and Wc is the total weight of starch and chitosan as constituents (g).

2.4. Characterization of Stc-EGDMA-Cts

2.4.1. FTIR Spectroscopy

FTIR spectrophotometer was used to characterize the functional groups in Stc-EGDMA-Cts across different Stc: Cts mass ratios. The results were evaluated against the functional groups present in starch, EGDMA, and chitosan. For FTIR analysis, Stc-EGDMA-Cts powder was processed with KBr at 25 ºC, formed into a pellet, and examined using FTIR over the range of 4000 to 500 cm^{-1}, with 45 scans per second and a resolution of 2.0 cm.

2.4.2. X-ray diffraction (XRD) analysis

XRD analysis was performed on starch, chitosan, and Stc-EGDMA-Cts at various Stc: Cts mass ratios. The instrument used a scattering angle (2θ) from 5 to 85º, a scanning speed of 0.2 deg s^{-1}, and a step size of 0.02 deg.

2.4.3. The study of the surface morphology

An SEM analysis examined the surface morphology of starch, chitosan, and Stc-EGDMA-Cts at various Stc: Cts mass ratios. The compounds were analyzed by fixing a few drops of their powder on the iron stub of the SEM coated with gold.

2.4.4. Zeta potential (ζ)

The zeta potential (ζ) of the dispersed material of Stc-EGDMA-Cts obtained from synthesis was measured by laser Doppler electrophoresis using a zeta potential analyzer ranging from -500 to +500 mV. The data were acquired in triplicate. Additionally, the zeta potential of wastewater containing Dypro 19 at pH 5, pH 7, and pH 8 was measured using the same instrument.

2.5. Flocculation experiments

2.5.1. Jar test

Jar test experiments were conducted to determine the effect of initial pH and Stc-EGDMA-Cts dosage in different mass ratios (Stc: Cts 0.5, 1, 2, 4, and 8 g g^{-1}) on the dye reduction from wastewater. The experiments were carried out on artificial wastewater by dissolving 0.25 g of Dypro 19 powder in water and then diluting it until 8 litres. A 500 ml dye solution was poured into a beaker glass and placed at the jar test instrument for flocculation experiments. The best initial pH level was determined by testing the textile dye wastewater at initial pH levels of 5, 6, 7, 8, and 9. In contrast, the amount of wastewater, Stc-EGDMA-Cts dosage, rapid mixing, gentle mixing, settling time, and temperature remained fixed at 500 mL, 2 mL L^{-1}, 200 rpm for 4 minutes, 30 rpm for 15 minutes, 60 minutes, and room temperature, respectively. The dosage optimization of Stc-EGDMA-Cts was conducted by varying dosages from 1.4 to 3.0 mL L^{-1}. On the other hand, the quantity of wastewater, initial pH, rapid mixing, gentle mixing, settling time, and temperature were maintained at 500 mL, the best initial pH, 200 rpm for 4 minutes, 30 rpm for 15 minutes, 60 minutes, and ambient temperature, respectively. Following establishing an optimum condition from the jar test, the sedimentation experiment was carried out with different settling times ranging from 0 to 1440 minutes. Ultimately, the settled flocs were examined using a digital microscope at 50 and 100 times magnification.

2.5.2. Dye analysis using UV-visible spectrophotometer and calculation of dye removal

Dye analysis was performed using a single-beam UV-visible spectrophotometer with a 1 cm quartz cuvette. The baseline and zeroing were corrected using demineralized water. The maximum absorbance of Dypro 19 was measured by scanning it in 400–800 nm wavelength ranges. The wavelength that resulted in maximum absorbance was used to measure the absorbance of the sample. The calibration curve for Dypro 19 was constructed using concentrations of 5, 10, 20, 30, 40, and 50 ppm. The limit of detection (LOD) and quantification (LOQ) were calculated using the linear regression of the calibration curve following Equations 2 and 3.

$$LoD = \frac{\sigma}{s} * 3 \qquad \text{(Eq.2)}$$

$$LoQ = \frac{\sigma}{s} * 10 \qquad \text{(Eq.3)}$$

where σ and s are the intercept standard deviation and the slope of the calibration curve, respectively. Furthermore, the percentage of dye removal can be calculated using Equation 4.

$$\text{Dye removal (\%)} = \frac{A_0 - A_t}{A_0} * 100 \qquad \text{(Eq.4)}$$

where A_0 is the dye absorption before treatment with Stc-EGDMA-Cts, and A_t is the absorption of dye after treatment with Stc-EGDMA-Cts.

3. Results and Discussion

3.1. Synthesis and characterization of Stc-EGDMA-Cts

Stc-EGDMA-Cts was synthesized through a free radical polymerization process under hydrothermal conditions. The synthesis process involves dissolving starch, chitosan, and AIBN initiator, followed by mixing, homogenization, and polymerization under hydrothermal conditions. The desired product was produced even though nitrogen purging was not carried out during the polymerization process. This synthesis method offers a simple and environmentally friendly approach. Although the AIBN initiator is classified as harmful, it is less toxic than the cerium ammonium nitrate used in a previous study [15]. The characteristics of Stc-EGDMA-Cts were determined using FTIR, XRD, SEM, and zeta potential. FTIR was used to determine the functional groups of Stc-EGDMA-Cts at various Stc: Cts mass ratios and compare them with the functional groups of the constituents (starch, chitosan, and EGDMA). Characterization using XRD was carried out to demonstrate the crystallinity of Stc-EGDMA-Cts at various Stc: Cts mass ratios, starch, and chitosan. SEM was used to evaluate the morphology of Stc-EGDMA-Cts at various Stc: Cts mass ratios and compare it with starch and chitosan as constituents. Zeta potential measurements were performed to determine the particle charge of Stc-EGDMA-Cts at various Stc: Cts mass ratios. Based on FTIR spectra in Fig 1a, the evidence found is: First, the functional groups of starch identified are OH, CH, CH_2, CH_3, and CO. A broad peak at 3284 cm-1 denotes the O-H stretching. The C-H stretching peaks at 2926 cm^{-1} (C-H) and 1337 cm^{-1} (C-H_2 and C-H_3). The 1148, 1077, and 995 cm-1 peaks suggested the C-O stretching. The FTIR also identified intramolecular H-bonding with carboxyl groups in the starch. The peak reveals it at 1641 cm^{-1}. The starch FTIR spectrum in Fig. 1a is similar to the FTIR spectra described by previous researchers [10,38,39]. Second, chitosan functional groups are identified as NH, OH, CH, and CO. The vibration mode at 3365, 3279, 2873, 1645, and 1023 cm^{-1} is N-H, O-H, C-H, C=O, and C-O stretching, respectively. The vibration mode at 1569 cm^{-1} and 1373 cm^{-1} is NH_2 and CH_2 bending. The intramolecular H-bonding with carboxyl groups and CH_3 deformation are indicated at 1645 cm^{-1} and 1373 cm^{-1}. The FTIR spectrum of chitosan in Figure 1a is identical to those observed in previous research [30,40–42]. Third, identified EDGMA functional groups are CH, C=O, C=C, and C-O. The vibration modes at 2959, 1716, and 1635 cm^{-1}, 1293 cm^{-1}, and 1143

cm^{-1} are C-H, C=O, C=C, and C-O stretching, respectively, while at 1450 cm^{-1} are CH_2 bending and CH_3 deformation. Finally, Stc-EGDMA-Cts shows peaks corresponding to its constituents' functional groups (starch, chitosan, and EGDMA), including OH, NH, CH, C=O, C=C, NH_2, CH_2, CH_3, and C-O. The vibration mode at 3304, 2930, 1724, 1637, and 1148 cm^{-1}, 1078 cm^{-1} and 1018 cm^{-1} is O-H and N-H, C-H, C=O, C=C, and C-O stretching, respectively, while the vibration mode at 1558 and 1449 cm^{-1} is NH_2 bending and CH_2 and CH_3 deformation.

The FTIR spectra of Stc-EGDMA-Cts at various Stc: Cts mass ratios are presented in Figure 1b. The spectral pattern shows a similar trend, indicating that the functional groups of Stc-EGDMA-Cts at various Stc: Cts mass ratios from 0.5 to 8 g g^{-1} are identical. A slight difference in intensity was observed in the characteristic absorption at 1558 cm-1, which showed the N-H group originating

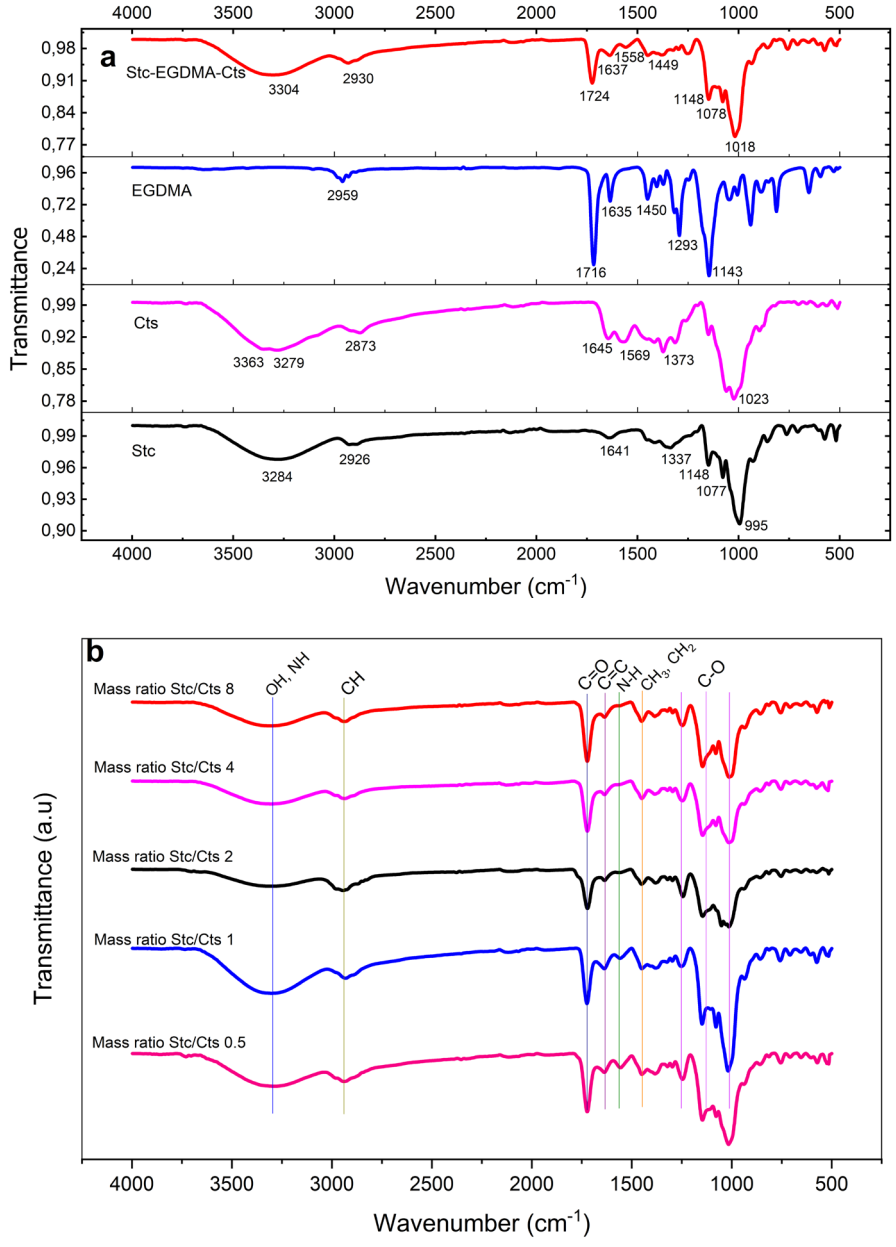

Fig. 1. (**a**) FTIR spectra of starch (Stc), chitosan (Cts), ethylene glycol dimethacrylate (EGDMA), Stc-EGDMA-Cts, and (**b**) Stc-EGDMA-Cts at various Stc:Cts mass ratios

from chitosan. The absorption band decreases as the Stc: Cts mass ratio increases. Starch's presence becomes more dominant than chitosan as the Stc: Cts mass ratios increase.

The XRD patterns in Figure 2a show a noticeable disparity in peak intensities among the component substances (starch, chitosan) and Stc-EGDMA-Cts at a Stc:Cts mass ratio of 0.5. Starch shows peaks at 14.5º, 16.9º, and 21.9º. Chitosan shows peaks at 20.2º, 31.6º, and 45.3º. Stc-EGDMA-Cts shows a peak at 16.7º. In terms of quality, starch has higher crystallinity compared to chitosan. The Origine Lab program processed data with smoothing and baseline correction to determine the crystallinity. The crystallinity of starch and chitosan is 97.25 and 73.68%, respectively. The XRD spectra of Stc-EGDMA-Cts in Figure 2b demonstrate that changing Stc:Cts mass ratio from 0.5 to 8 g g^{-1} does not cause a noticeable change in the peak spectra pattern. Nevertheless, there was a minor variation in the

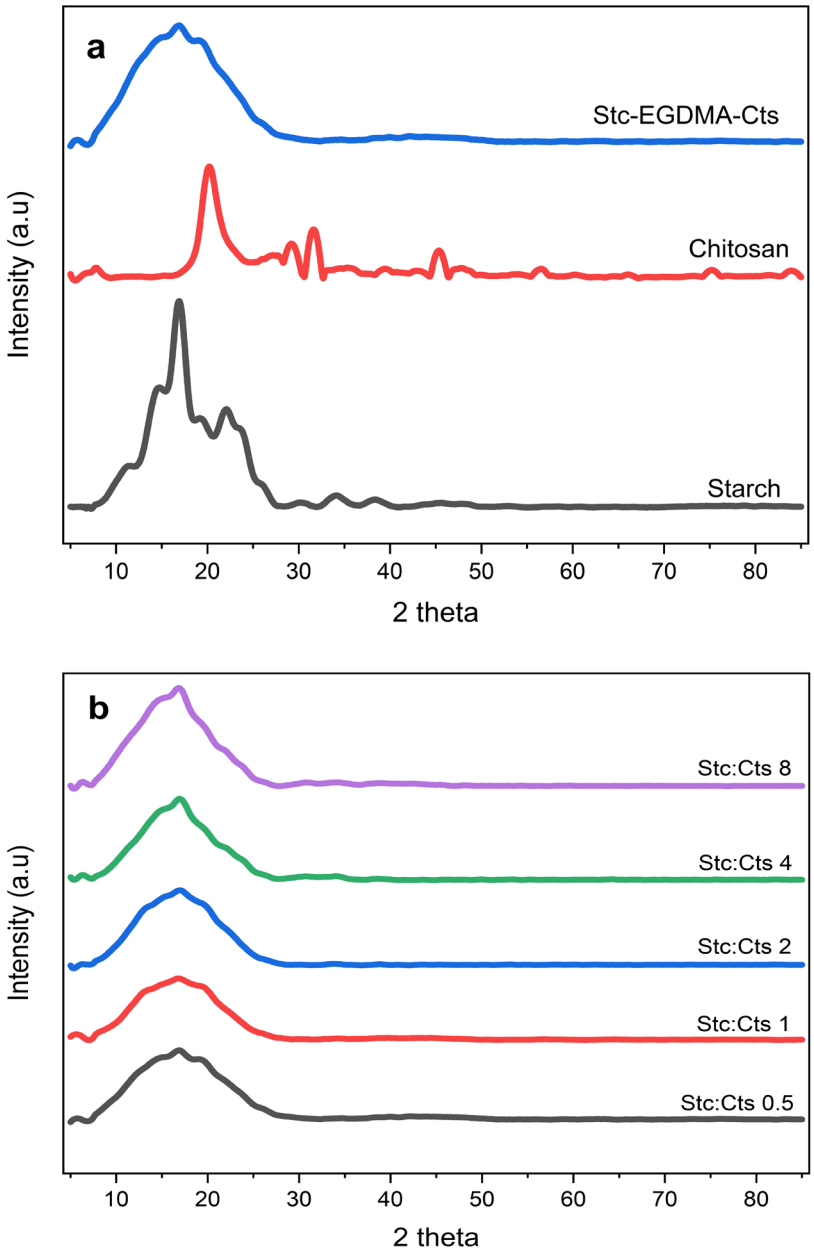

Fig. 2. (**a**) XRD spectra of starch (Stc), chitosan (Cts), Stc-EGDMA-Cts and (**b**) Stc-EGDMA-Cts at various Stc:Cts mass ratios

crystallinity of Stc-EGDMA-Cts at varying Stc:Cts mass ratios. Stc-EGDMA-Cts crystallinity was 95.68, 95.73, 99.99, 96.55, and 95.61% at Stc:Cts mass ratios of 0.5, 1.0, 2.0, 4.0, and 8.0 g g^{-1}, respectively. The XRD analysis results were confirmed by SEM investigation. Figure 3 presents SEM photos of starch, chitosan, and Stc-EGDMA-Cts at various Stc:Cts mass ratios. The SEM photos show that the surface of Stc-EGDMA-Cts at Stc:Cts mass ratios of 0.5, 1, 2, and 4 g g^{-1} is rougher than Stc:Cts mass ratio of 8 g g^{-1}. Stc-EGDMA-Cts has a rougher and larger surface than starch and chitosan, facilitating a better adsorption process. Stc:Cts mass ratio influences the percent yield and the zeta potential value of Stc-EGDMA-Cts. Table 1 shows that as the Stc:Cts mass ratio increases from 0.5 to 8 g g^{-1}, the percent yield rises from 15.64 to 59.93%, and the zeta potential increases from 21.3 to 46.4 mV. These results indicate that increasing the Stc:Cts mass ratios from 0.5 to 8 g g^{-1} produces Stc-EGDMA-Cts with longer and larger molecular structures. A long molecular structure with a high molecular charge promotes its function as a suitable flocculant. The molecule allows the bridging mechanism between particles to produce large flocs, facilitating the sedimentation process of the flocs. However, if the molecule is too long and large, it can reduce flocculation activity because of insolubility. This study demonstrated poor flocculant activity by Stc-EGDMA-Cts at a Stc:Cts mass ratio of 8 g g^{-1}.

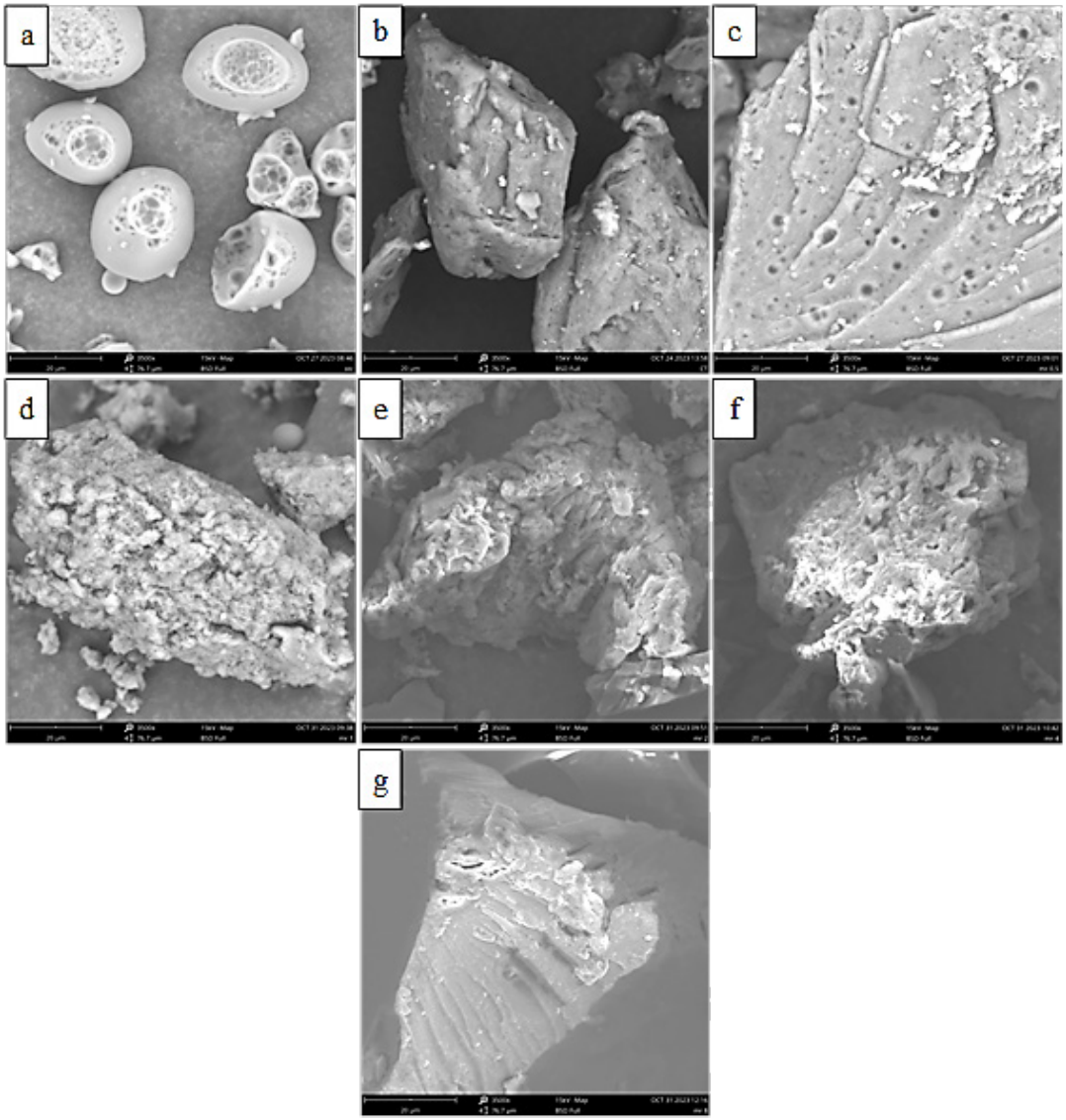

Fig. 3. SEM photos at 3,500 times magnification of starch (**a**), chitosan (**b**), and Stc-EGDMA-Cts at Stc:Cts mass ratio of 0.5 (**c**), 1 (**d**), 2 (**e**), 4 (**f**), and 8 (**g**)

Table 1. The percent grafting and the zeta potential of Stc-EGDMA-Cts at various Stc:Cts mass ratios

Stc:Cts mass ratio (g g^{-1})	Grafting (%)	Zeta potential (mV)
0.5	15.64 ± 13.21	23.1 ± 0.0
1.0	34.73 ± 21.99	30.2 ± 0.0
2.0	49.71 ± 21.74	40.1 ± 0.1
4.0	54.19 ± 12.14	42.3 ± 0.0
8.0	59.93 ± 12.41	46.4 ± 0.2

3.2. The performance of Stc-EGDMA-Cts in removing dye from wastewater

Stc-EGDMA-Cts performance in removing Dypro 19 from wastewater is evaluated using a UV-visible spectrophotometer. The absorbance of Dypro 19 standard solution and the standards calibration curve are presented in Figure 4. The maximum absorbance of Dypro 19 was measured at 588 nm (Fig. 4a). LOD and LOQ were determined from linear regression of standard calibration curve Y=0.0114*X + 0.00472, with the intercept standard deviation (σ) of 0.00425 (Fig. 4b). The LOD and LOQ values were found to be 1.12 and 3.73 mg L^{-1} (ppm), respectively. The highest and the lowest absorbance values observed in the flocculation performance test were 0.3435 and 0.019, respectively, corresponding to concentration values of 29.72 and 1.25 mg L^{-1} (ppm). Consequently, the measured concentrations remain above the LOD.

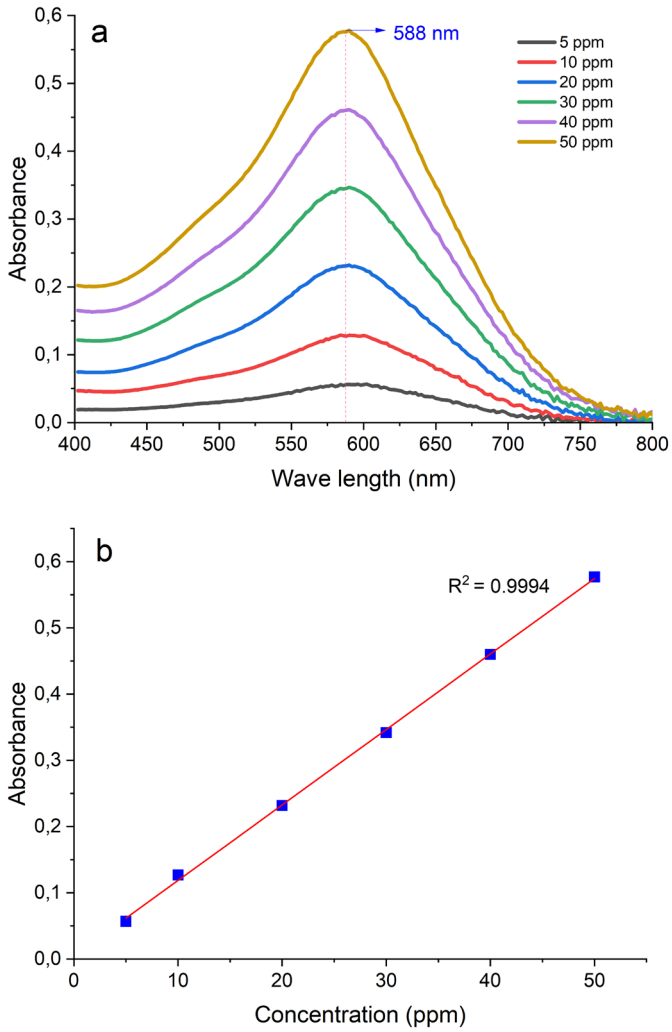

Fig. 4. UV spectra of standards solution (a), standards curve (b)

The performance of Stc-EGDMA-Cts at a certain Stc:Cts mass ratio (g g^{-1}) in removing Dypro 19 depends on the initial pH. Figure 5a shows that the best Stc-EGDMA-Cts performance is at an initial pH of 9, 8, 7, and 5 with Stc: Cts mass ratios of 0.5, 1, 2, and 4 g g^{-1}, respectively. The highest percentage of Dypro 19 removal achieved under these circumstances was 86.82, 76.47, 80.11, and 76.80%, respectively. At a Stc:Cts mass ratio of 8 g g^{-1}, Stc-EGDMA-Cts performance was poor, as it only reduced the Dypro 19 by less than 20%. According to the data presented in Figure 5a, it is possible that the best performance of Stc-EGDMA-Cts at a Stc:Cts mass ratio of 8 g g^{-1} is at a pH below 5. The optimum performance of Stc-EGDMA-Cts at various Stc:Cts mass ratios, which is highly dependent on an initial pH as described, is supported by the fact that the higher the value of the mass ratio of Stc:Cts, the more positive the zeta potential value of Stc-EDGMA-Cts. Conversely, the zeta potential value becomes more negative as the pH value of wastewater containing Dypro 19 decreases. Therefore, Stc-EGDMA-Cts at a larger mass ratio will achieve optimal flocculation performance at a low wastewater pH and vice versa. The dose is one of the critical factors in the coagulation-flocculation process, in addition to pH and mixing. The effect of the Stc-EGDMA-Cts dosage on removing Dypro 19 was investigated at various Stc:Cts mass ratios (0.5, 1, 2, and 4 g g^{-1}) under an optimum initial pH condition, as illustrated in Figure 5b. The optimum dosage was obtained at the highest percent dye removal. The optimum dosage for Stc:Cts mass ratios of 0.5, 1, 2, and 4 g g^{-1} is 2.0, 1.6, 2.4, and 2.0 mL L^{-1}, respectively, resulting in the percent dye removal of 91.01, 92.26, 92.84, and 80.85%, respectively. Figure 5c shows that the floc deposition time of the destabilized Dypro 19 was rapid enough. Deposition times of 15, 30, and 60 minutes resulted in dye removal of 91.06, 93.56, and 96.60%, respectively. From 60 to 1440 minutes, the dye removal rate remained relatively constant. This condition indicates that the generated flocs from the destabilization process of Dypro 19 from wastewater by Stc-EGDMA-Cts are relatively dense, heavy, and large, making them easy to settle quickly. Based on the graph in Figure 5a and Figure 5b, the optimum initial pH and the optimum dosage range obtained by Stc-EGDMA-Cts at mass ratio Stc:Cts 0.5, 1, 2, and 4 g g^{-1} is relatively narrow. Those suggest that the flocculation mechanism is the neutralization of particle charge. Below an optimum initial pH and dosage value, particle charge neutralization has yet to occur, resulting in stable dye particles. Above an optimum initial pH and an optimum dosage value, excess dosage and OH may cause a reversal of the day particle charge, leading to their stability.

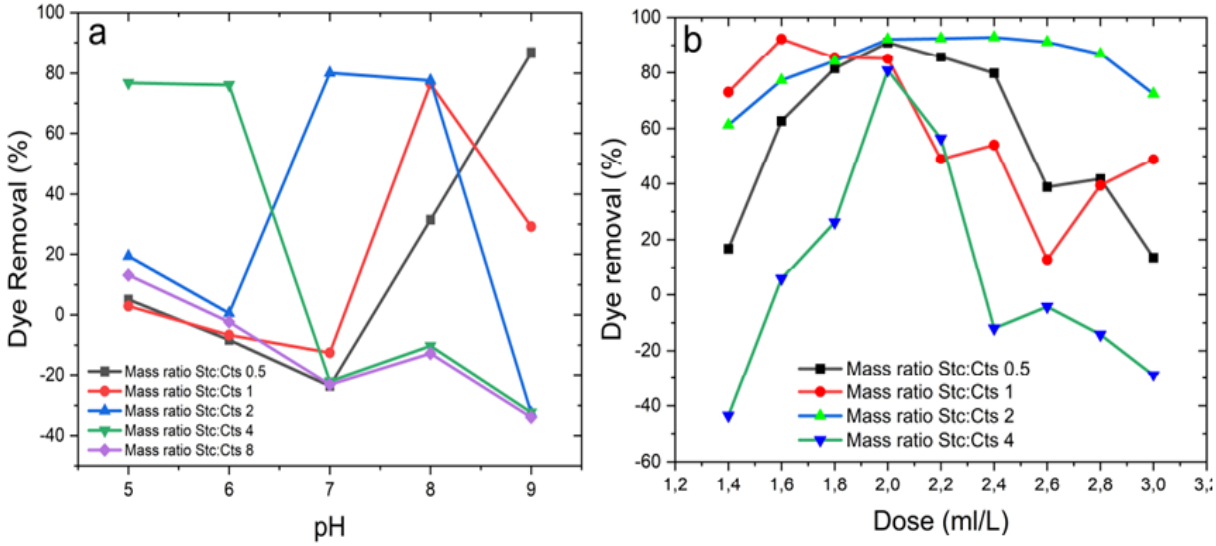

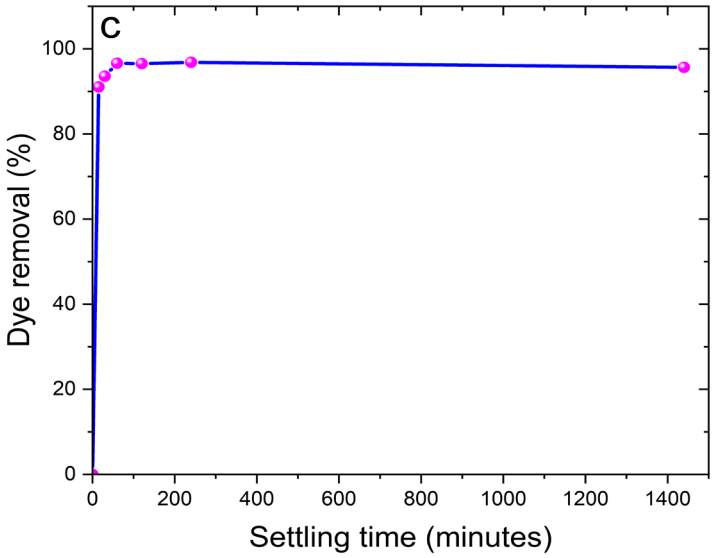

Fig. 5. The performance of Stc-EGDMA-Cts in removing Dypro 19 at various pH (**a**), at various doses (**b**), and settling time of destabilized Dypro 19 by STc-EGDMA-Cts (**c**)

The zeta potential value indicates the particle charge. Figure 6 illustrates the zeta potential value of Stc-EGDMA-Cts at Stc:Cts mass ratios of 1, 2, and 4 g g^{-1}, as well as the Dypro 19 wastewater pH. The zeta potential values indicate that particle charge neutralization is one of the mechanisms of Dypro 19 particle destabilization by Stc-EGDMA-Cts. In addition to adsorption and charge neutralization, the flocculation mechanism by Stc-EGDMA-Cts involves polymer bridging. The flocs image in Figure 7 shows floc sizes larger than 100 µm, indicating that polymer bridging has occurred between destabilized dye particles. This bridging causes the flocs to agglomerate, making them settle quickly.

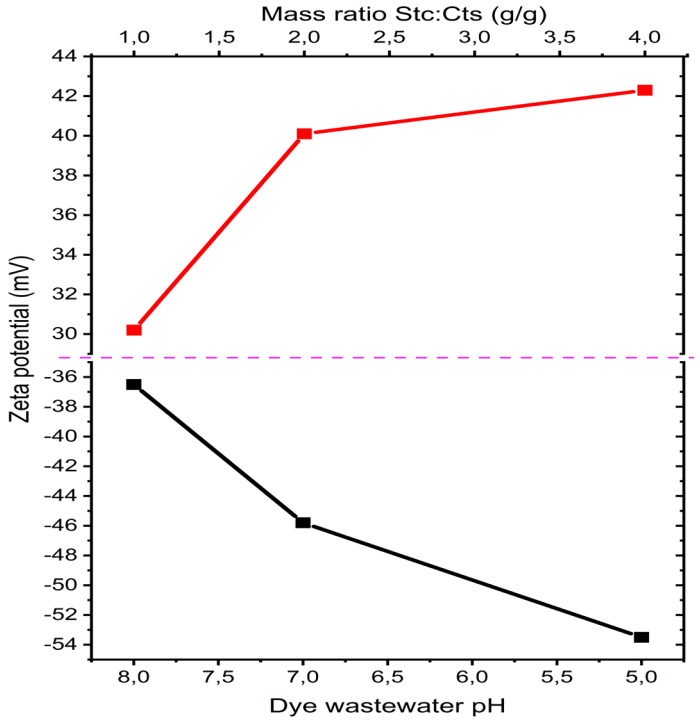

Fig. 6. Zeta potential values of Stc-EGDMA-Cts and the Dypro 19 wastewater before flocculation

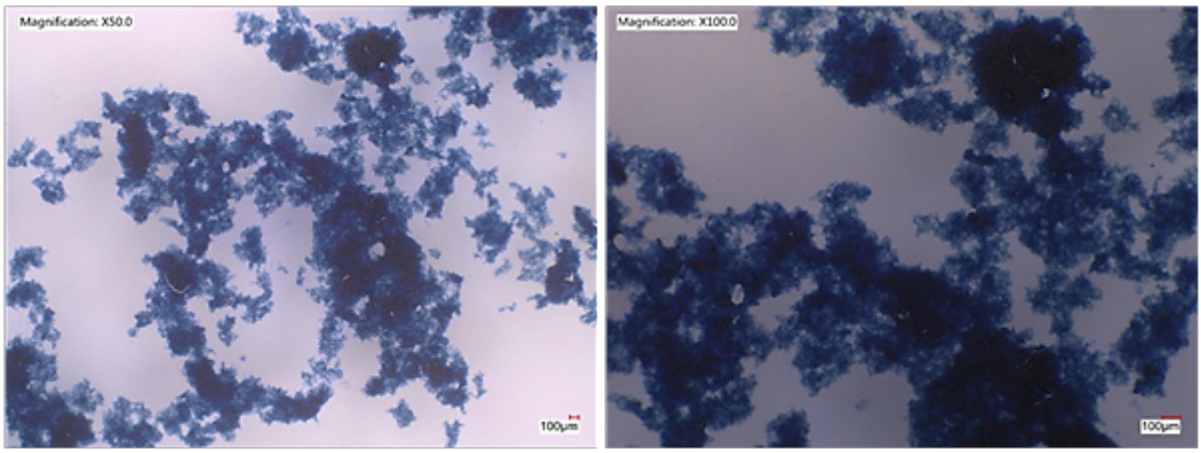

Fig. 7. The flocs image of Dypro 19 destabilized by Stc-EGDMA-Cts flocculant

4. Conclusion

Stc-EGDMA-Cts, a natural polymer-based flocculant, has been successfully synthesized simply and environmentally friendly through free radical polymerization under hydrothermal conditions without purging nitrogen gas. The mass ratio of Stc:Cts (g g^{-1}) influences the characteristics of the synthesized Stc-EGDMA-Cts and its performance in removing dye from wastewater. The mass ratio of Stc:Cts from 0.5 to 8 g g^{-1} increased the percent yield and the zeta potential value of the Stc-EGDMA-Cts. The Stc-EGDMA-Cts at mass ratios of 0.5 to 8.0 g g^{-1} have similar functional groups, high crystallinity, and qualitatively rougher and larger surface area than starch and chitosan. The performance of Stc-EGDMA-Cts at various Stc:Cts mass ratios in removing dyes above 80% evaluated by a UV-visible spectrophotometer method was determined by a specific pH, a specific flocculant dosage, a floc size, and settles quickly. Based on the results of characterization and flocculation performance tests, Stc-EGDMA-Cts was found to employ charge neutralization, adsorption, and polymer bridging as mechanisms for dye flocculation.

5. Acknowledgements

The authors would like to thank The Research Organization of Life Sciences and Environment, The National Research and Innovation Agency (BRIN), Indonesia, for funding this research under the scheme of Rumah (Home) Program 2023 for the Results of the Disclosure and Utilization of Indonesian Biodiversity. There are no conflicts of interest to disclose.

6. References

[1] E. Hogue, The Importance of Water Quality, National Ocean Service, 2021. https://sanctuaries.noaa.gov/news/aug21/water-quality-month.html (accessed June 13, 2024)

[2] M. Arjomandi, A review: Analytical methods for heavy metals determination in environment and human samples, Anal. Methods Environ. Chem. J. (2019) 97–126. https://doi.org/10.24200/amecj.v2.i03.73

[3] S. Teimoori, A.H. Hassani, M. Panahi, New extraction of toluene from water samples based on nano-carbon structure before determination by gas chromatography, Int. J. Environ. Sci. Technol., 20 (2023) 6589–6608. https://doi.org/10.1007/s13762-023-04906-9

[4] R. Ashouri, A.M. Rashidi, S.A.H. Mirzahosseini, N. Mansouri, Dynamic and static removal of benzene from air based on task-specific ionic liquid coated on MWCNTs by sorbent tube-headspace solid-phase extraction procedure, Int. J. Environ. Sci. Technol., 18 (2021) 2377–2390. https://doi.org/10.1007/s13762-020-02995-4

[5] S. Teimoori, A.H. Hassani, M. Panahi, Rapid

extraction of BTEX in water and milk samples based on functionalized multi-walled carbon nanotubes by dispersive homogenized-micro-solid phase extraction, Food Chem., 421 (2023) 136229. https://doi.org/10.1016/j.foodchem.2023.136229

[6] S. Teimoori, M. Panahi, N. Mansouri, An immobilization of aminopropyl trimethoxysilane-phenanthrene carbaldehyde on graphene oxide for toluene extraction and separation in water samples, Chemosphere, 316 (2023) 137800. https://doi.org/10.1016/j.chemosphere.2023.137800

[7] C.S. Lee, J. Robinson, M.F. Chong, A review on application of flocculants in wastewater treatment, Process Saf. Environ. Prot., 92 (2014) 489–508. https://doi.org/10.1016/j.psep.2014.04.010

[8] X. Jiang, Y. Li, X. Tang, J. Jiang, Q. He, Z. Xiong, H. Zheng, Biopolymer-based flocculants: a review of recent technologies, Environ. Sci. Pollut. Res., 28 (2021) 46934–46963. https://doi.org/10.1007/s11356-021-15299-y

[9] Y. Sun, D. Li, X. Lu, J. Sheng, X. Zheng, X. Xiao, Flocculation of combined contaminants of dye and heavy metal by nano-chitosan flocculants, J. Environ. Manage., 299 (2021) 113589. https://doi.org/10.1016/j.jenvman.2021.113589

[10] L. You, F. Lu, D. Li, Z. Qiao, Y. Yin, Preparation and flocculation properties of cationic starch/chitosan crosslinking-copolymer, J. Hazard. Mater., 172 (2009) 38–45. https://doi.org/10.1016/j.jhazmat.2009.06.120

[11] C.S. Lee, J. Robinson, M.F. Chong, A review on application of flocculants in wastewater treatment, Process Saf. Environ. Prot., 92 (2014) 489–508. https://doi.org/10.1016/j.psep.2014.04.010

[12] H. Zhang, G. Guan, T. Lou, X. Wang, High performance, cost-effective and ecofriendly flocculant synthesized by grafting carboxymethyl cellulose and alginate with itaconic acid, Int. J. Biol. Macromol., 231 (2023) 123305. https://doi.org/10.1016/j.ijbiomac.2023.123305

[13] C. Zhao, J. Zhou, Y. Yan, L. Yang, G. Xing, H. Li, P. Wu, M. Wang, H. Zheng, Application of coagulation/flocculation in oily wastewater treatment: A review, Sci. Total Environ., 765 (2021) 142795. https://doi.org/10.1016/j.scitotenv.2020.142795

[14] M.A.A. Razali, A. Ariffin, Polymeric flocculant based on cassava starch grafted polydiallyldimethylammonium chloride: Flocculation behavior and mechanism, Appl. Surf. Sci., 351 (2015) 89–94. https://doi.org/10.1016/j.apsusc.2015.05.080.

[15] J. Xun, T. Lou, J. Xing, W. Zhang, Q. Xu, J. Peng, X. Wang, Synthesis of a starch–acrylic acid–chitosan copolymer as flocculant for dye removal, J. Appl. Polym. Sci., 136 (2019) 47437. https://doi.org/10.1002/app.47437

[16] S.Y. Choy, K.M.N. Prasad, T.Y. Wu, M.E. Raghunandan, R.N. Ramanan, Utilization of plant-based natural coagulants as future alternatives towards sustainable water clarification, J. Environ. Sci., 26 (2014) 2178–2189. https://doi.org/10.1016/j.jes.2014.09.024

[17] S. Mohd Asharuddin, N. Othman, W.A.H. Altowayti, N. Abu Bakar, A. Hassan, Recent advancement in starch modification and its application as water treatment agent, Environ. Technol. Innov., 23 (2021) 101637. https://doi.org/10.1016/j.eti.2021.101637

[18] N. Das, N. Ojha, S.K. Mandal, Wastewater treatment using plant-derived bioflocculants: green chemistry approach for safe environment, Water Sci. Technol., 83 (2021) 1797–1812. https://doi.org/10.2166/wst.2021.100

[19] J. Bendoraitiene, E. Lekniute-Kyzike, R. Rutkaite, Biodegradation of cross-linked and cationic starches, Int. J. Biol. Macromol., 119 (2018) 345–351. https://doi.org/10.1016/j.ijbiomac.2018.07.155

[20] B. Zaman, N. Hardyanti, M. Arief Budiharjo, S. Budi Prasetyo, A. Ramadhandi, A. Tri

Listiyawati, Natural flocculant VS chemical flocculant where is better to used in Wastewater treatment, IOP Conf. Ser. Mater. Sci. Eng., 852 (2020) 12014. https://doi.org/10.1088/1757-899X/852/1/012014

[21] J. El-Gaayda, F.E. Titchou, R. Oukhrib, P.-S. Yap, T. Liu, M. Hamdani, R. Ait Akbour, Natural flocculants for the treatment of wastewaters containing dyes or heavy metals: A state-of-the-art review, J. Environ. Chem. Eng., 9 (2021) 106060. https://doi.org/10.1016/j.jece.2021.106060

[22] M. Nasrollahzadeh, M. Sajjadi, S. Iravani, R.S. Varma, Starch, cellulose, pectin, gum, alginate, chitin and chitosan derived (nano)materials for sustainable water treatment: A review, Carbohydr. Polym., 251 (2021) 116986. https://doi.org/10.1016/j.carbpol.2020.116986

[23] T.G. Ambaye, M. Vaccari, S. Prasad, E.D. Van Hullebusch, S. Rtimi, Preparation and applications of chitosan and cellulose composite materials, J. Environ. Manage., 301 (2022) 113850. https://doi.org/10.1016/j.jenvman.2021.113850

[24] S.A. Ishak, M.F. Murshed, H. Md Akil, N. Ismail, S.Z. Md Rasib, A.A.S. Al-Gheethi, The application of modified natural polymers in toxicant dye compounds wastewater: A review, Water (Basel), 12 (2020) 2032. https://doi.org/10.3390/w12072032

[25] V.H. Dao, N.R. Cameron, K. Saito, Synthesis, properties and performance of organic polymers employed in flocculation applications, Polym. Chem., 7 (2016) 11–25. https://doi.org/10.1039/C5PY01572C

[26] C. Feng, Y. Li, D. Yang, J. Hu, X. Zhang, X. Huang, Well-defined graft copolymers: from controlled synthesis to multipurpose applications, Chem. Soc. Rev., 40 (2011) 1282–1295. https://doi.org/10.1039/B921358A

[27] M.Á. Vega-Hernández, G.S. Cano-Díaz, E. Vivaldo-Lima, A. Rosas-Aburto, M.G. Hernández-Luna, A. Martinez, J. Palacios-Alquisira, Y. Mohammadi, A. Penlidis, A review on the synthesis, characterization, and modeling of polymer grafting, Processes, 9 (2021) 375. https://doi.org/10.3390/pr9020375

[28] S.S. Ngema, A.K. Basson, T.S. Maliehe, Synthesis, characterization and application of polyacrylamide grafted bioflocculant, Phy. Chem. Earth, Parts A/B/C, 115 (2020) 102821. https://doi.org/10.1016/j.pce.2019.102821

[29] H. Wu, Z. Liu, A. Li, H. Yang, Evaluation of starch-based flocculants for the flocculation of dissolved organic matter from textile dyeing secondary wastewater, Chemosphere, 174 (2017) 200–207. https://doi.org/10.1016/j.chemosphere.2017.01.120

[30] D. Wang, T. Zhao, L. Yan, Z. Mi, Q. Gu, Y. Zhang, Synthesis, characterization and evaluation of dewatering properties of chitosan-grafting DMDAAC flocculants, Int. J. Biol. Macromol., 92 (2016) 761–768. https://doi.org/10.1016/j.ijbiomac.2016.07.087

[31] M.T. ALSamman, J. Sánchez, Recent advances on hydrogels based on chitosan and alginate for the adsorption of dyes and metal ions from water, Arab. J. Chem., 14 (2021) 103455. https://doi.org/10.1016/j.arabjc.2021.103455

[32] L. Zhang, Y. Zeng, Z. Cheng, Removal of heavy metal ions using chitosan and modified chitosan: A review, J. Mol. Liq., 214 (2016) 175–191. https://doi.org/10.1016/j.molliq.2015.12.013

[33] Y. Zhang, M. Zhao, Q. Cheng, C. Wang, H. Li, X. Han, Z. Fan, G. Su, D. Pan, Z. Li, Research progress of adsorption and removal of heavy metals by chitosan and its derivatives: A review, Chemosphere, 279 (2021) 130927. https://doi.org/10.1016/j.chemosphere.2021.130927

[34] A. Apriyanto, J. Compart, J. Fettke, A review of starch, a unique biopolymer – Structure, metabolism and in planta modifications, Plant. Sci., 318 (2022) 111223. https://doi.org/10.1016/j.plantsci.2022.111223

[35] N.J. Arsad, N. Ngadi, S.F. Mohamed Razak, Preparation of chitosan-grafted nanocellulose via microwave-initiate method, Appl. Mech. Mater. 818 (2016) 281–284. https://doi.org/10.4028/www.scientific.net/AMM.818.281

[36] L. Qiao, S. Wang, T. Wang, S. Yu, S. Guo, K. Du, High-strength and low-swelling chitosan/cellulose microspheres as a high-efficiency adsorbent for dye removal, Cellulose, 28 (2021) 9323–9333. https://doi.org/10.1007/s10570-021-04111-2

[37] T.Adali,E.Yilmaz,Synthesis,characterization and biocompatibility studies on chitosan-graft-poly(EGDMA), Carbohydr. Polym., 77 (2009) 136–141. https://doi.org/10.1016/j.carbpol.2008.12.017

[38] N. Alvarado, R.L. Abarca, J. Urdaneta, J. Romero, M.J. Galotto, A. Guarda, Cassava starch: structural modification for development of a bio-adsorber for aqueous pollutants. Characterization and adsorption studies on methylene blue, Polymer Bull., 78 (2021) 1087–1107. https://doi.org/10.1007/s00289-020-03149-9

[39] A. Hebeish, A.A. Aly, A. El-Shafei, S. Zaghloul, Synthesis and characterization of cationized starches for application in flocculation, finishing and sizing, Egypt. J. Chem., 52 (2009) 0449-2285. https://ejchem.journals.ekb.eg/

[40] E.S. de Alvarenga, Characterization and properties of chitosan, biotechnology of biopolymers, InTech Publisher book, 2011. https://doi.org/10.5772/17020

[41] A. Drabczyk, S. Kudłacik-Kramarczyk, M. Głąb, M. Kędzierska, A. Jaromin, D. Mierzwiński, B. Tyliszczak, Physicochemical investigations of chitosan-based hydrogels containing Aloe Vera designed for biomedical use, Materials, 13 (2020) 3073. https://doi.org/10.3390/ma13143073

[42] S. Yasmeen, M. Kabiraz, B. Saha, Md. Qadir, Md. Gafur, S. Masum, Chromium (VI) ions removal from tannery effluent using chitosan-microcrystalline cellulose composite as adsorbent, Int. Res. J. Pure Appl. Chem., 10 (2016) 1–14. https://doi.org/10.9734/IRJPAC/2016/23315